

Spectrum Estimation and Noise Reduction for Laser Induced Breakdown Spectroscopy

Yuanping Chen, A. M. Yusuf, Liang Wang, and Hansheng Zhang

Department of Electrical and Computer Engineering

Mississippi State University

Mississippi State, Mississippi 39762

ABSTRACT

Laser Induced Breakdown Spectroscopy (LIBS) is a well-known technique to measure certain atomic and molecular in various environment. A pulsed laser beam (532nm) is focused with a lens to the target, which can be gas, liquid, or solid to induce a micro-plasma in the focal area. The induced plasma is of very high temperature (about 10,000K). Any material in the plasma is excited and it produces strong optical emission. Spectroscopy analysis of the emission gives information about the properties of the material present in the laser induced plasma. The emission signal collected is embedded with background noise mainly due to instrumentation.

In this paper, three algorithms based on adaptive line enhancer, autocorrelation and low pass filter were used to effectively extract the noise embedded signal, the SNR improvement has been obtained for three methods. The eigenanalysis frequency estimation method was used to determine the minimum number of data samples required to get a stable frequencies output [1].

1. INTRODUCTION

Laser Induced Breakdown Spectroscopy (LIBS) is a laser-based, non-intrusive, and highly sensitive optical diagnostic technique. Soon after the development of the ruby laser, it was reported in 1963 that by focusing the laser beam, the breakdown of air could be caused [2,3]. A very bright spot, which is similar to a discharge spark between two electrodes, was observed in the focal point region. Therefore, the laser induced breakdown is defined as the generation of a practically ionized gas (plasma) by a laser pulse. The laser induced breakdown plasma produces a strong optical emission. The

spectroscopy analysis of the emission gives information about the properties of the material present in the laser breakdown plasma.

LIBS has several advantages over other conventional methods of atomic emission spectroscopy. The focused laser beam provides spatial resolution. The point measurement permits the study of homogeneity of the target sample. Solid, liquid and gaseous material can be excited. The laser pulse vaporizes and excites the sample in one simple step. Elaborate sample preparation and auxiliary equipment are not needed. Being an emission method, LIBS provides simultaneous multielement analysis capabilities when using an optical multichannel analyzer (OMA). Since the spark can be generated at a remote location, analysis can be performed in situ in harsh or dangerous environments. Only optical access to the medium being sampled is required. Early studies concentrated on sparks in simple gases such as air [4], hydrogen[5], helium[6--9], and argon[10]. These results showed that when the plasma formed in the laser breakdown spark (< 100 ns), the electron density is greater than the electrode spark. In 1983 Radziemski et al.[11] reported their research of time-resolved LIBS in aerosols. They used a Q-switched Nd:YAG laser operating at 1.06 μm to generate the laser induced plasma. Comparing the experimental data with the calculations, they concluded the plasma acts as if it were in local thermodynamic equilibrium after 1 ms. They also performed two experiments on an experimental coal gasification system and obtained real-time spectral information. Because of the advantages of a laser probe, LIBS soon was introduced into the combustion diagnostics research field. Schmieder[12] applied LIBS to a coaxial air/methane/air diffusion flame by creating a series of sparks along a radius just above the burner. The spark spectrum for each position was recorded. From the relative intensities of the carbon, nitrogen, hydrogen, and oxygen lines, the fuel/

air ratio as a function of position was obtained. In 1989 Ottesen et al.[13] developed a system to provide in situ determination of size, velocity and elemental composition for individual particles in combustion environments. Laser sparks were produced by single particle with the use of a Q-switched Nd:YAG laser, and time-resolved emission spectra were observed. Their results indicated a high sensitivity of the technique to mineral matter in coal particles.

The LIBS spectrum usually is very noisy. The noise comes from many different mechanisms, which include dark current of the detector, heat noise of the detector and electric circuit, stray light in the spectrograph, the continuous radiation of the plasma, and the serious fluctuation in the emission intensity which is influenced by the plasma propagation in the form of shock wave. Sometimes, especially in field test, the influence of the environment such as site vibration and unexpected light also induces some noise. Reducing the noise is an important aspect in the instrumental development. The recent trend of diagnostic technique is *on site* analysis. Low noise and quick response are becoming more and more important.

2. EXPERIMENTAL APPARATUS AND DATA COLLECTION

2.1. A.experimental apparatus

The LIBS experimental apparatus consisted of four main equipments: laser, signal receiver, spectral analyzer, and sample generator. Figure 1 shows the diagram of the laboratory LIBS system. The heart of the system was a Q-switched Nd:YAG laser (Continuum surelite II). The laser output was at 1064 nm or at 532 nm after frequency doubling. The pulse width was 10 ns with a maximum repetition rate of 10 Hz. The maximum output energy was 700 mJ at 1064 nm or 300 mJ at 532 nm. In most of the experiments, the 532 nm beam at energy levels from 100 to 200 mJ was used. The laser beam was delivered by a series of right angle turning-prisms to a table in an adjacent laboratory. A 20 cm focal length lens was used to focus the laser beam to the sample area to form the induced plasma. The LIBS signal was collected perpendicular to the laser beam. A lens of 15 cm focal length and 7.5 cm in diameter was used to collect the LIBS signal. The signal was coupled to the optical fiber through another lens of 5 cm focal length. An optical fiber coupler on the other end of the fiber was used to couple the signal to the spectrograph. The spectrograph was a 0.5 m HR460 with a 2400 line/mm grating. An EG&G Princeton Applied Research Corporation (PARC) diode array detector with a 1024 pixel was mounted on the exit of the spectrograph. The detector was controlled by an EG&G PARC 1427 Multichannel Detector Controller. A spectral region of

about 20 nm was covered simultaneously with this configuration. A high voltage pulse generator was used to control the time delay and gate width of the detector. The LIBS signal was recorded and stored in a PC.

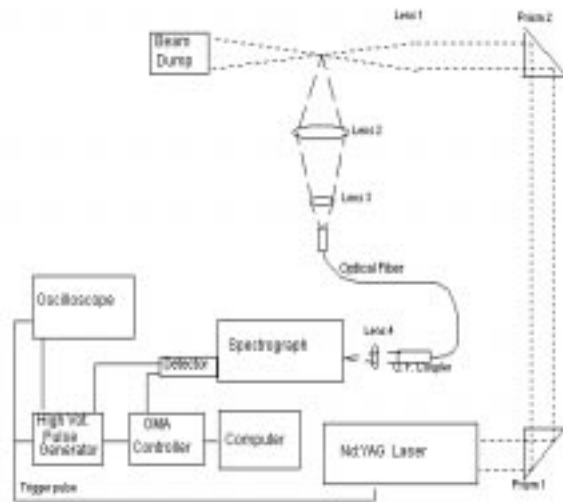


Fig. 1. Diagram of LIBS system

2.2. Data collection

As an initial study of applying DSP technique to LIBS spectra, a set of 30 spectra of element Cr at the spectral region around 360 nm was recorded. The sample solution was 2 ppm Cr in a 1% HCl solution. It was pumped through a tubing pump into a nebulizer to generate dry aerosol. The aerosol blows out through a tube of 0.5 inch in diameter. The laser beam was focused 3mm about the tube. The diode array detector was gated at 10ms delay and 5 ms width. The detector exposure time was 30 ms, and the sample time was 500 ms. Considering the software set up time, this sample time allowed to record one spectrum through two laser shots. Since the intensity fluctuation was very serious, for about one third of the 30 spectra, it's difficult to distinguish the three Cr spectral lines from noise, for about another one third of the 30 spectra, the three Cr line were clear, and for another one third, the three Cr line were ambiguous. This set of 30 spectra were used as a test data for digital signal processing.

3. III. ALGORITHMS

3.1. ALE algorithm

Filtering has been with us for a long time. Long time ago, man has attempted to remove the more visible of the impurities in his water by filtering, and one

dictionary gives a first meaning for the none filter as "a contrivance for freeing liquids from suspended impurities, especially by passing them through strata of sand, charcoal, etc."

Modern usage of the word filter often involves more abstract entities than fluids with suspended impurities. There is usually however the notion of something passing a barrier: one speaks of news filtering out of the war zone, or sunlight filtering through the trees. Sometimes the barrier is interposed by man for the purpose of sorting out something that is desired from something else with which it is contaminated. One example is of course provided by water purification; the use of an ultraviolet filter on a camera provides another example. When the entities involved are signals, such as electrical voltages, the barrier--in the form perhaps of an electric network--becomes a filter in the sense of signal processing.

Filters were originally seen as circuits or systems with frequency selective behavior. The series or parallel tuned circuit is one of the most fundamental such circuits in electrical engineering, and as a "wave trap" was a crucial ingredient in early crystal sets. More sophisticated versions of this same idea are seen in the IF strip of most radio receivers; here, tuned circuits, coupled by transformers and amplifiers, are used to shape a passband of frequencies which are amplified, and a stopband where attenuation occurs.

The usual method of estimating a signal corrupted by additive noise is to pass the composite signal through a filter that tends to suppress the noise while leaving the signal relatively unchanged. The design of such filters is the domain of optimal filtering, which originated with the pioneering work of Wiener and was extended and enhanced by the work of Kalman, Bucy, and others [14-18].

Filters used for the foregoing purpose can be fixed or adaptive. The design of fixed filters must be based on prior knowledge of both the signal and the noise, but adaptive filters have the ability to adjust their own parameters automatically, and their design requires little or no prior knowledge of signal or noise characteristics.

Noise cancelling is a variation of optimal filtering that is highly advantageous in many applications. It uses an auxiliary or reference input derived from one or more sensors located at points in the noise field where the signal is weak or undetectable. This input is filtered and subtracted from a primary input containing both signal and noise. As a result, the primary noise is attenuated or eliminated by cancellation.

Sometimes subtracting the noise from a received signal would seem dangerous. If done improperly it could result in an increase in output noise power. If the

filtering and subtraction are controlled by an appropriate adaptive process, noise reduction can in many cases be accomplished with little risk of distorting the signal or increasing the output noise level. In circumstances where adaptive noise canceling is applicable, we can often achieve a degree of noise rejection that would be difficult or impossible to achieve by direct filtering.

Some of the earliest work in adaptive interference canceling was performed by Howells and Applebaum and their colleagues at the General Electric Company between 1957 and 1960. They designed and built a system for antenna sidelobe canceling using a reference input derived from an auxiliary antenna and a simple two-weight adaptive filter [19].

At the time of this early work, only a handful of people were interested in adaptive systems, and the development of the multiweight adaptive filter just beginning. In 1959, Widrow and Hoff at Stanford University were devising the Least-Mean-Square (LMS) adaptive algorithm and the pattern recognition scheme known as Adaline (for "adaptive linear threshold logic element") [20, 21]. Aizermann and his colleagues were constructing an automatic gradient searching machine [22]. In Great Britain, D. Gabor and his associates were developing adaptive filters [23]. Each of these efforts was proceeding independently.

In the early and middle 1960s, work on adaptive systems intensified. Hundreds of papers on adaptation, adaptive controls, adaptive filtering, and adaptive signal processing appeared in the literature. An important commercial application of adaptive filtering in digital communications grew from the work during this period of Lucky at the Bell Laboratories [24, 25].

In 1965 an adaptive noise-canceling system was built at Stanford University. Its purpose was to cancel the 60-hertz interference at the output of an electrocardiographic amplifier and recorder.

Since 1965 adaptive noise canceling has been successfully applied to a number of additional problems, including other aspects of electrocardiography, the elimination of periodic interference in general [26], and the elimination of echoes on long-distance telephone transmission lines [27, 28].

Adaptive Line Enhancement (ALE) is a development of the adaptive noise cancellation method. In this application, the adaptive algorithm is directed towards the problem of enhancing one or more narrowband signals of unknown and possibly drifting amplitudes and frequencies which are embedded in narrowband noise. The ALE system is depicted in Figure 2.

This system, which was introduced by Widrow et al [29], uses the measured signal at the desired response

and a delayed version of itself as input. Suppose the signal $d(n)$ consists of two components: a narrowband component that has long-range correlations such as a sine wave, and a broadband component which will tend to have short--range correlations [30].

The principle is that the delay should decorrelate the noise while leaving the narrowband components correlated. When functioning in an ideal way, the adaptive filter output is an enhanced version of the sinusoidal components. It is the filter output $y(n)$ which is the required output.

Figure 2 illustrates a block diagram of the adaptive line enhancer, where a delayed version of the input signal is used as an input to the adaptive filter whose coefficients are adapted to best fit the portion of the input signal which is uncorrelated with the noise, i.e. the noise-free signal portion of the input, by minimizing the mean squared error. The filter output is an enhanced version of the input.

The computational Algorithm for the ALE is [31]

$$y(n) = \sum_{m=0}^L f_m(n)x(n-m) \quad (1)$$

$$x(n) = d(n - \Delta) \quad (2)$$

$$e(n) = d(n) - y(n) \quad (3)$$

$$f_m(n+1) = f_m(n) + 2\mu e(n)x(n-m) \quad (4)$$

A direct implementation of the algorithm requires a prior knowledge of delay factor D , which is also known as the decorrelation parameter, the adaptation parameter μ , and the filter length L .

Adaptive Line Enhancer is a method of optimal filtering that can be applied whenever a suitable reference input is available. The principal advantage of the method are its adaptive capability, its low output noise, and its low signal distortion. The adaptive capability allows the processing of inputs whose properties are unknown and in some cases nonstationary. It leads to a stable system that automatically turns itself off when no improvement in the signal-to-noise ratio can be achieved. The output noise and signal distortion are generally lower than that achievable with conventional optimal filter configurations [32] [33].

3.2. B. Autocorrelation algorithm

Correlation technique is used widely in communications, instrumentations, computers,

telemetry, sonar, radar and other signal processing systems. Correlation has several desirable properties, including

1. The ability to detect a desired signal in the presence of noise or other signals.
2. The ability to recognize specific patterns within analog or digital signals.
3. The ability to measure time delays through various media, such as materials, the human body, RF paths, electronic circuits, etc.

As these properties indicate, correlation is essentially a comparison process. In fact, we use correlation daily when we compare sounds, imagines, or other sensations relative to other sounds, imagines, or sensations stored in our brain. The key function of the human comparison process is to measure mentally the degree of similarity between two or more parameters. Generally, this sort of comparison is capable of discriminating extraneous forms of information and noise from a given seneum. The comparison can be made in real time, or we can mentally store the data until some later time.

The mental correlation process works well where the decision making process is not limited by time constraints. However, in electronic systems we do not usually have the luxury of performing correlation at our leisure. Correlation must be performed in real time, requiring the use of electronic circuits that compatible with the system in question.

The formula for autocorrelation algorithm is as below:

$$y(n) = \sqrt{\frac{1}{L} \sum_{k=0}^{L-1} x(n)x(n+k)} \quad (5)$$

In our case, the principle for autocorrelation is not complicated. In frequency domain, the signal response for LIBS spectrum is narrow banded, but the distribution for noise spectrum is wide banded. The autocorrelation algorithm can decorrelate the noise signal and leave the true signal unchanged (or just changed a little bit, due to the spectrum bandwidth expansion). There is one parameter in this algorithm should be selected, the correlation factor L , if L is too large, that will lead to wide bandwidth of true signal; if L is too small, we can not achieve desired Signal to Noise Ratio (SNR) improvement. So parameter L should be carefully chosen both to improve the SNR and not to deform the true signal.

3.3. C. FIR linear phase low pass filter algorithm.

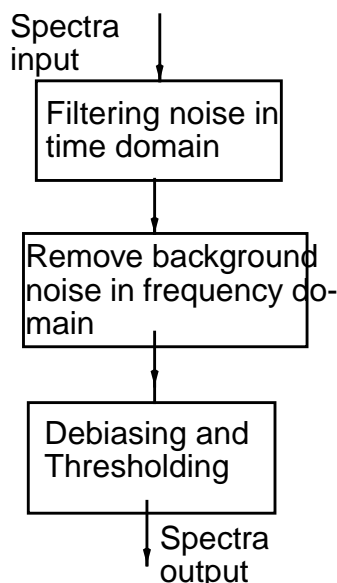


Fig. 3. Low pass filter algorithm

Fig. 3 shows the flow chart of FIR linear phase low pass filter algorithm.

By observing data, we note that the spectrum signal in time axis (corresponding to each channel) is low frequency signal, and noise is random and high frequency signal compared to spectrum signal. So, we may design a low pass filter to pass spectrum signal and attenuate noise in the time axis for each channel. There is one more thing needed to be taken into account, and that is spectrum amplitude distortion problem. The spectrum amplitude in time axis represents spectrum density in different time, and this is a parameter that is not tolerant of distortion. Based on above observations, we choose a linear phase low pass filter to process the spectrum signal in time axis.

An FIR filter of length M has a frequency response

$$H(\omega) = \sum_{k=0}^{M-1} b_k e^{-j\omega k} = \sum_{k=0}^{M-1} h(n) e^{-j\omega k} \quad (6)$$

In symmetry condition and antisymmetry condition, a FIR filter has linear phase.

For symmetry condition,

$$h(n) = h(M-1-n) \quad (7)$$

For antisymmetry condition,

$$h(n) = -h(M-1-n), \quad (8)$$

The choice of a symmetric or antisymmetric unit sample response depends on the application. An antisymmetric FIR filter is not suitable as a lowpass filter because $H(0)=0$. Consequently, we would not use the antisymmetric condition in the design of a lowpass linear-phase FIR filter. On the other hand, the symmetry condition yields a linear phase FIR filter with a nonzero response at $\omega=0$. So, the symmetry condition lends itself to low pass filter. The frequency response of an FIR filter having a unit sample response $h(n)$ that satisfies the symmetry condition may be expressed as

$$H(\omega) = H_r(\omega) e^{-j\omega \frac{(M-1)}{2}} \quad (8)$$

where

$$H_r(\omega) = h\left(\frac{M-1}{2}\right) + 2 \sum_{n=0}^{\frac{(M-3)}{2}} h(n) \cos \omega(M-1-n) \quad (9)$$

for M of odd

$$H_r(\omega) = 2 \sum_{n=0}^{\frac{M}{2}-1} h(n) \cos \omega\left(\frac{M-1}{2}-n\right) \quad (10)$$

for M of even

$$\Theta(\omega) = -\omega\left(\frac{M-1}{2}\right) \quad (11)$$

If we specify the frequency response at $M/2$ points in ω , above $H_r(\omega)$ equation constitutes $dM/2e$ linear equation for determining the coefficients $\{h(n)\}$ of an linear phase FIR filter. Although the values of ω can be chosen arbitrarily, it is usually desirable to select equally spaced points in frequency, in the range $0 < \omega < \pi$. Then how to choose the values of $H_r(\omega)$ is the key of designing linear phase filter, and it depends on the design specification. If $H_r(\omega)$ change abruptly from the passband, where $H_r(\omega_k) = 1$, to the stopband, where $H_r(\omega_k) = 0$, it will lead to large sidelobes in the stopband. Instead of having an abrupt change, if we

specify an intermediate value for $H_r(w)$ in the transition region, the resulting frequency response has significantly smaller sidelobes in the stopband. The only disadvantage is that the width of the transition region is increased. However, the benefits usually outweigh the one disadvantage. Further reduction in the stopband sidelobes can be obtained by allowing for one or more additional frequency specifications in the transition band. In effect, the transition band is widened further to achieve additional reduction in the stopband sidelobes.

The question that we have not addressed is concerned with the values of the specifications in the transition band. This problem has been considered in the technical literature by Rabiner, et al. (1970) [34]. In this paper the optimum values of the specification in the transition region are tabulated for a large variety of filter lengths. The values given are optimum in the sense that they result in minimizing the largest sidelobe in the stopband. These tables are available in Appendix C of the textbook.

We choose $M=15$, $BW=1$, and $T1=0.43378296$ from Table C.1 in textbook [35], and the corresponding linear phase FIR filter has the band width of $2p/15$, the transition region width of $2p/15$, and the maximum sidelobe of -42.30932283 dB. $H(w_k) = \{1, 0.43378296, 0, 0, 0, 0, 0, 0\}$. Run matlab command

$$b = \text{fir2}(n, f, m) \quad (12)$$

where b is the vector of FIR coefficients $h(n)$, n is the length of the FIR filter, f is the vector of frequency points, and m vector is the amplitude values of frequency points, or $H(w_k)$. we get

$$h(n) = \{0.0003, 0.0012, 0.0059, 0.0198, 0.0471, 0.0835, 0.1159, 0.1289, 0.1159, 0.0835, 0.0471, 0.0198, 0.0059, 0.0012, 0.0003\}. \quad (13)$$

Then, we use a c program to implement this FIR filter, and process spectrum data in the time axis for each channel.

In fig. 9, we note that high frequency noise rides on a low frequency background noise in frequency domain. If the background noise is removed, it is clearly that the signal to noise ratio will be increased. we design a moving average low pass filter to remove the background noise. The moving average filter is defined by the difference equation

$$y(n) = \frac{1}{M+1} \sum_{n=0}^M x(n-k) \quad (14)$$

Clearly, moving average system is a linear phase FIR filter with impulse response

$$h(n) = \frac{1}{M+1}, \quad (15)$$

Its linear phase characteristic is very important because it prevents background noise from distortion.

After removing background noise, debias the DC component, and threshold negative value.

3.4. D. Eigenanalysis frequency estimation

The spectral frequency estimation is processed in three step. Fig. 4 is the flow chart of this processing

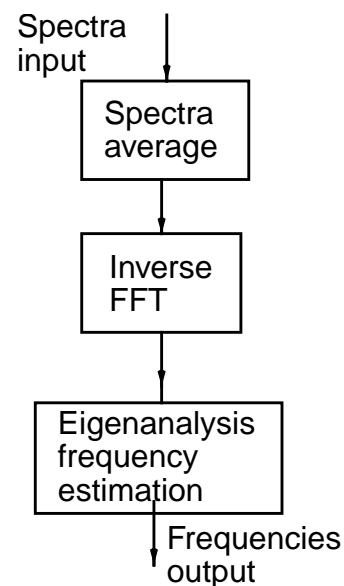


Fig. 4. Eigenanalysis frequency estimation

Recent exiting technique is to average 30-50 single spectrum to get a quality spectrum. The purpose of this processing is to find out how the average number affect the estimation result. The 30 test spectra is averaged at the number one through thirty, and every different averaged spectrum is further processed.

The spectrum is taken by the spectrograph, and it's a signal of frequency domain. In order to perform eigenanalysis frequency estimation, the spectra signal needs to be back to time domain, and so inverse FFT algorithm is applied.

The Fourier transform is the mathematical foundation

for relating a time or space signal to its frequency domain representation.

To perform inverse Fourier transform, a complex number is required. The test spectra are real data series. It is set as a real component of the complex number and the imaginary component of the complex number is set to zero.

Then subroutine of Eigenanalysis frequency estimation is called to perform frequency estimation. The following is the brief description of eigenanalysis frequency estimation [36] [37].

The basis for the improved performance of the eigenanalysis techniques is the division of the information in the autocorrelation matrix or the data matrix into two vector subspaces, one a signal subspace and the other a noise subspace.

Functions of the vectors in either the signal or noise subspaces can be used to create frequency estimators that, when plotted, show sharp peaks at the frequency locations of sinusoidal or other narrowband spectral components. These are not true PSD estimators because they do not preserve the measured process power nor can the autocorrelation sequence be recovered by Fourier transforming the frequency estimator. Included in this class of eigenanalysis-based frequency estimators are the Pisarenko harmonic decomposition (PHD) and the multiple signal classification (MUSIC) algorithms.

It was known that if the process consists of M real sinusoidal in additive real white noise, the ACS is

$$\sum_{i=1}^M \frac{P_i}{2} [e^{j2\pi f_i kT} + e^{-j2\pi f_i kT}] + Q_w \zeta[k] \quad (16)$$

in which P_i is the power of the i th sinusoidal and r_w is the noise variance.

In an analogous manner, the p th-order autocorrelation matrix for the case of M real sinusoidal in white noise has the structure

$$R_p = \sum_{i=1}^M \frac{P_i}{2} [s_i s_i^H + s_i s_i^T] + Q_w I \quad (17)$$

The signal matrix S_p in this case will have rank $2M$. Discussions from this point will concentrate on the complex case; the real case is generally a simple extension of the complex case with a change in rank M to $2M$.

The signal matrix will have the eigendecomposition

$$S_p = \sum_{i=1}^{P+1} \lambda_i v_i v_i^H \quad (18)$$

Thus the eigenvectors V_{M+1}, \dots, V_{P+1} span the noise subspace of R_p , all with the identical eigenvalue r_w . The principal eigenvectors V_1, \dots, V_M span the signal subspace of both R_p and S_p , with eigenvalues of $\lambda_1 + r_w, \dots, \lambda_M + r_w$.

The eigenvalues of the principal eigenvectors, though, are composed of powers of both signal and noise so white noise does not contribute to the eigenvalue weighing of the noise-free signal subspace eigenvectors.

The eigendecomposition of the autocorrelation matrix can be exploited in two ways to generate improved spectral estimators, or more correctly, improved frequency estimators. Retaining only the information in the signal subspace eigenvectors, that is, forming a lower-rank approximation to R_p , effectively enhances the SNR because of the omission of the contribution of power in the noise subspace components. This is the basis of principal component (signal subspace) frequency estimators. Noting that the eigenvectors are orthogonal and that the principal eigenvectors span the same subspace of the signal vectors, then the signal vectors are orthogonal to all the vectors in the noise subspace, including any linear combination

$$S_i^H \sum_{k=M+1}^{p+1} a_k v_k = 0 \quad (19)$$

for $1 < i < M$ (or $2M$ in the case of M real sinusoidal). This property forms the basis of the noise subspace frequency estimators.

The autocorrelation sequence normally is not known, so that the above properties are mostly of theoretical, rather than practical, interest. The concepts, however, can be extended to the covariance and modified covariance data matrices that are a part of the exponential estimation techniques of the Prony method. It is shown in this section that the data matrices have eigendecomposition properties similar to the autocorrelation matrix. The principal eigenvectors of the data matrix predominantly span the signal subspace and the singular values of these principal eigenvectors tend to be larger than the noise subspace singular values. Thus the singular values determined by a SVD of the data matrix are the basis for the separation of the eigenvectors into a mostly signal subspace and a mostly noise subspace.

The Prony method was introduced as a technique for the estimation of the parameter of a damped exponential model that approximates a given data sequence. Central to the method is the solution $T_p H T_p$ in which T_p is the order p data matrix of the covariance method of linear prediction

$$T_p = \begin{bmatrix} x[p+1] & \cdots & x[1] \\ \vdots & \ddots & \vdots \\ x[N] & \cdots & x[N-p] \end{bmatrix} \quad (20)$$

The modified Prony method, a variation of the Prony method for undamped sinusoidal modeling, involves the modified covariance data matrix

$$\begin{bmatrix} T_p \\ T_p^* J \end{bmatrix} \quad (20) \quad (21)$$

the discussion which follows will focus on matrix T_p , but the conclusions will also be valid for the modified covariance data matrix

The discussion which follows will focus on matrix T_p , but the conclusions will also be valid for the modified covariance data matrix.

Consider the noiseless complex exponential signal sequence

$$x[n] = \sum_{k=1}^M h_k z_k^n \quad (22)$$

in which $z_k = \exp([\alpha_k + j 2\pi f_k]T)$ and $h_k = A_k \exp(jF_k)$. Note that damped exponential are permitted as valid signals. Matrix T_p formed from the $x[n]$ will have rank M as long as the selected order p is within the range $M \leq p \leq N-M$ (for the modified covariance matrix the range is $M \leq p \leq [N-M]/2$). The data matrix T_p can be decomposed as

$$T_p = BC \quad (23)$$

in which B an $(N-p) \times M$ matrix and C , and $M \times p$ matrix, are

Then we get

$$T_p H T_p = C^H B^H BC \quad (24)$$

The related $M \times M$ matrix $B^H B C C^H$ is positive definite because both B and C have full rank M . If l_i for $1 \leq i \leq M$ designates the eigenvalues, then

$$(C^H B^H BC) w_i = l_i w_i \quad (25)$$

for $1 < i < M$. Premultiply the above Eq by matrix C^H to yield

$$(C^H B^H B C C^H) w_i = l_i C^H w_i \quad (26)$$

Define the vector

$$v_i = C^H w_i \quad (27)$$

and with proper substitution it leads to the result

$$T_p H T_p v_i = l_i v_i \quad (28)$$

for $1 \leq i \leq M$. The M nonzero eigenvalues of the $p \times p$ matrix $T_p H T_p$ are there identical to the eigenvalues of the matrix $B^H B C C^H$. The remaining $p-M$ eigenvalues of $T_p H T_p$ are zero because $T_p H T_p$ is of rank M . The corresponding eigenvectors of the nonzero eigenvalues are given. Thus any principal eigenvector of $T_p H T_p$ will be a linear combination of the columns of C^H , which is composed of signal vectors as shown above. It can also be shown that any principal eigenvector of $T_p H T_p$ is a linear combination of the columns of B , which is also composed of signal vectors. The matrix T_p will have M nonzero singular values, as these simply the square roots of the eigenvalues. The eigenvectors of the zero eigenvalues of $T_p H T_p$ or $T_p T_p^H$ are orthogonal to the M signal subspace, or principal, eigenvectors associated with the nonzero eigenvalues in the signal subspace.

If the data has noise, the properties are not exactly true, but they tend to be approximately true. Thus, the M principal singular values of a T_p matrix composed of noisy samples tend to be larger than the $p - M$ smallest singular values (which were exactly zero in the noiseless case). The M eigenvectors corresponding to the M principal eigenvalues of either $T_p H T_p$ or $T_p T_p^H$ have fewer noise contributions than the noise subspace eigenvectors corresponding to the $p - M$ smallest singular values. These statements have some justifications as a result of the analysis provided earlier.

It has been shown that retention of the signal subspace or principal, eigenvectors effectively improves the SNR for processes consisting of exponential in white noise by eliminating much of the noise contribution to an

autocorrelation matrix or a data matrix.

Consider the correlation method PSD estimator, the minimum variance PSD estimator, and the Yule-Walker autoregressive PSD estimator, The correlogram and MV methods rely on the known or estimated autocorrelation matrix R_p for the definition of the spectral estimate

$$P_{CORR}(f) = T e^H(f) R_p e(f) \quad (29)$$

$$P_{MV}(f) = T [e^H(f) R_p^{-1} e(f)]^{-1} \quad (30)$$

while the autoregressive (AR) method depends on the autocorrelation matrix to obtain the AR parameters

$$\begin{bmatrix} 1 \\ a_p \end{bmatrix} = R_p^{-1} \begin{bmatrix} Q_p \\ O_p \end{bmatrix} \quad (31)$$

where the vectors and matrix have the following definitions

$$T_P = \begin{bmatrix} r_{xx}[0] & \dots & r_{xx}[p] \\ r_{xx}[p] & & r_{xx}[0] \end{bmatrix} \quad (32)$$

$$e(f) = \begin{bmatrix} 1 \\ e^{(j2\pi fT)} \\ e^{j2\pi f pT} \end{bmatrix} \quad (33)$$

If the orthogonal eigendecomposition of R_p is

$$R_p = \sum_{k=1}^P \lambda_k v_k v_k^H \quad (34)$$

in which the eigenvalues are ranked in decreasing magnitude $\lambda_1, \lambda_2, \dots, \lambda_p$ and there are estimated to be M principal components ($M < p$) then the reduced rank principal eigenvector approximation to R_p and R_p^{-1}

$$R_p = \sum_{k=1}^M \lambda_k v_k v_k^H \quad (35)$$

$$R_p^{-1} = \sum_{k=1}^M \frac{1}{\lambda_k} v_k v_k^H \quad (36)$$

may be used in lieu of R_p and R_p^{-1} in the above equations to create spectral estimators with reduced noise contribution due to the omission of the noise subspace eigenvectors.

The simple idea of separating eigenvectors into signal and noise subspaces based upon an examination of either the eigenvalues of the autocorrelation matrix or the singular values of the data matrix does not work well in practice, especially with short sample records. The AIC order-selection criterion first introduced has been extended to handle the subspace separation problem. Assuming $\lambda_0, \lambda_1, \dots, \lambda_p$ are the eigenvalues of the sample autocorrelation matrix R_p and assuming $m < p$, where m is the number of sinusoidal signals actually present in the data, and N data samples, then

$$AIC[m] = \quad (37)$$

$$(p-m) \ln \left[\frac{\frac{1}{p-m} \sum_{i=m+1}^P \lambda_i}{\prod_{i=m+1}^P \lambda_i^{-(p-m)}} \right] + (m(2p-m))$$

The number of sinusoidal in the signal subspace is determined by selecting the minimum value of $AIC[m]$. Wax and Kailath[1986] have reported some preliminary results from use of the criterion of the above equation.

4. IV. RESULTS AND DISCUSSION

4.1. Evaluation method

Use mean square signal to noise ratio to evaluate the system.

$$SNR = 10 \log \left(\frac{\frac{1}{NM} \sum_{i=1}^N \sum_{j=1}^M Signal[i][j]^2}{\frac{1}{NQ} \sum_{i=1}^N \sum_{j=1}^Q Noise[i][j]^2}} \right) \quad (38)$$

where $\text{Signal}[i][j]$ stand for signals, $\text{Noise}[i][j]$ stand for noise, i indexes time axis frame, and j indexes channel number of frequency domain.

4.2. Autocorrelation Scheme

Figure 3 is one set of original data collected by the LIBS system, the 3 central peaks represent three signals, this spectrum is strongly corrupted by the noise.

In order to remove the noise from the signal, we applied autocorrelation algorithm. Figure 4 is the output of this algorithm, compared with the original data, some of the random noise has been removed. In this application, we selected correlation length $L=3$, because if L is larger, the output spectrum will be broadened, that will lead to spectrum distortion. In this application, autocorrelation is a good approach.

4.3. Adaptive Line Enhancer

Figure 5 is the output of the adaptive line enhancer, we select filter length $L=30$, a value can be selected from a wide range. When a is larger than 10^{-5} , this algorithm will not converge, so this is not the desired result. When a is smaller than 10^{-9} , that will cause slow convergence and strong spectrum distortion. In this application, we choose $a=5 \cdot 10^{-7}$, the output of ALE will reduce the noise level but introduce some distortion near the spectrum lines. Although ALE system can achieve SNR improvement in this application, but it is not as desirable as we expected.

4.4. Low Pass Filter Scheme

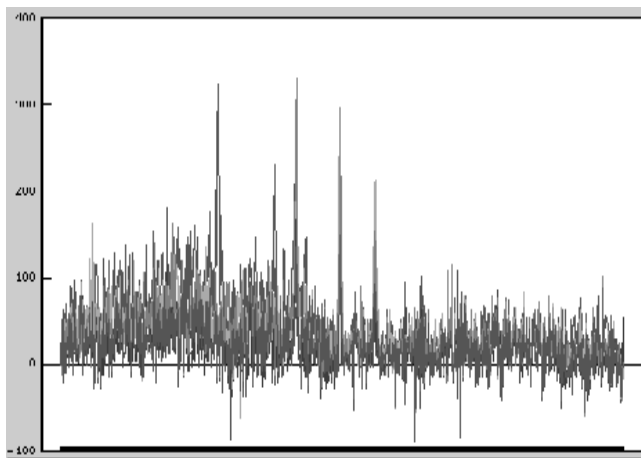
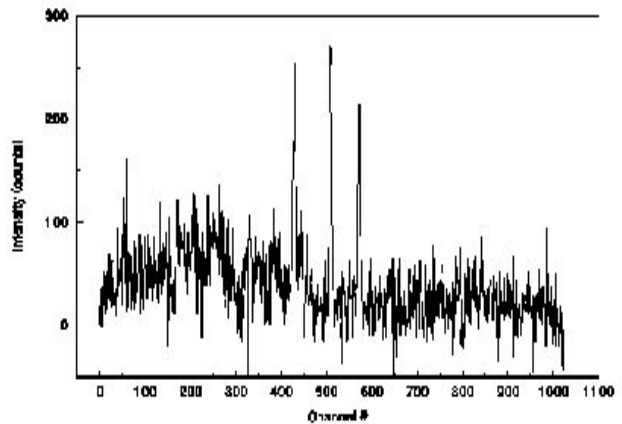


Fig. 8. Six overlapped original spectra

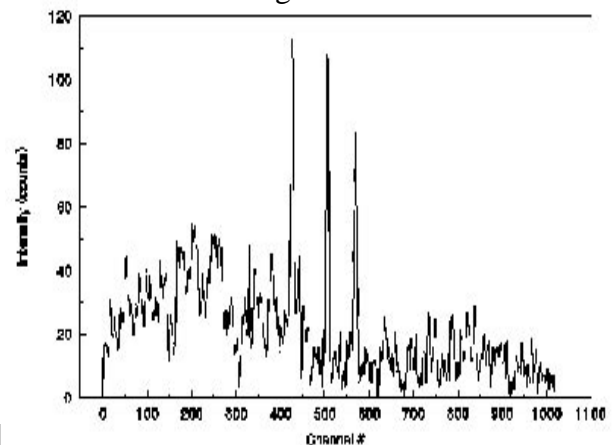
The fig. 8 is original overlapped spectra in six successive time points and the fig. 9 is the

LIBS Original Spectrum (set 15)
Fig. 5



Result of Autocorrelation

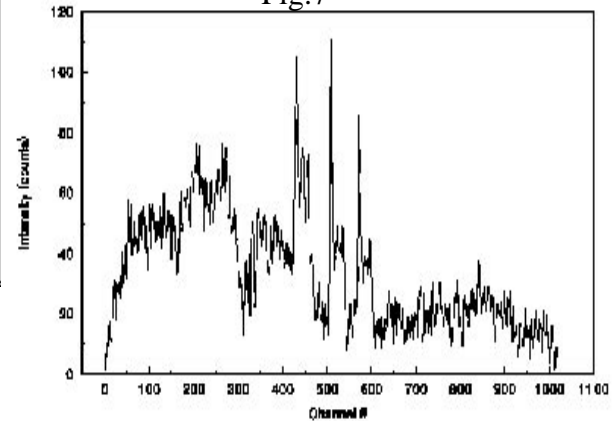
Fig. 6



Result of Adaptive Line Enhancer

$\alpha=5 \cdot 10^{-7}$, $L=30$

Fig. 7



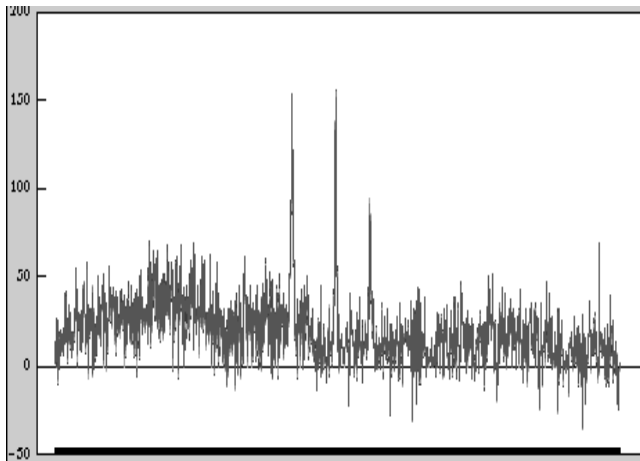


Fig. 9. Six overlapped processed spectra

corresponding processed spectra obtained by time domain low pass filtering. From these two figures, we can see that processed signals are much better than original signals. In processed spectra, we note that the three peaks in the middle and one peak in the right are signals, while in the original spectra, some noise peaks are higher than signal peaks, and you can not distinguish signal and noise.

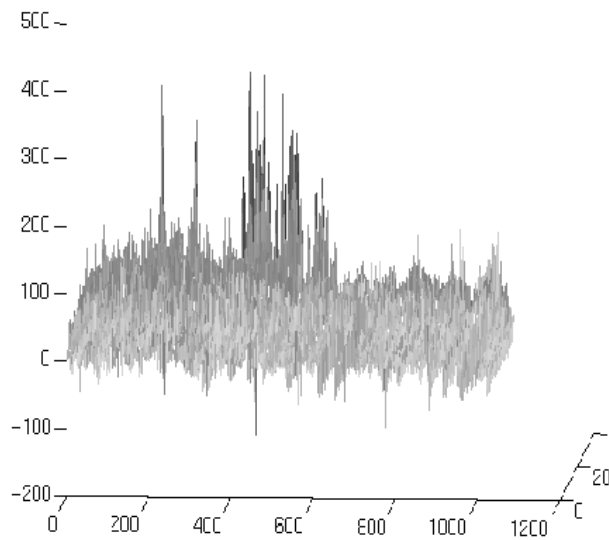


Fig. 10. 3_D original spectra

Fig. 10 is the original spectra plotted in 3_D. Fig. 11 is processed spectra obtained by low pass filter algorithm. Comparing both figures, it is obvious that processed spectra are greatly improved in term of signal to noise ratio.

4.5. Eigenanalysis Frequency Estimation

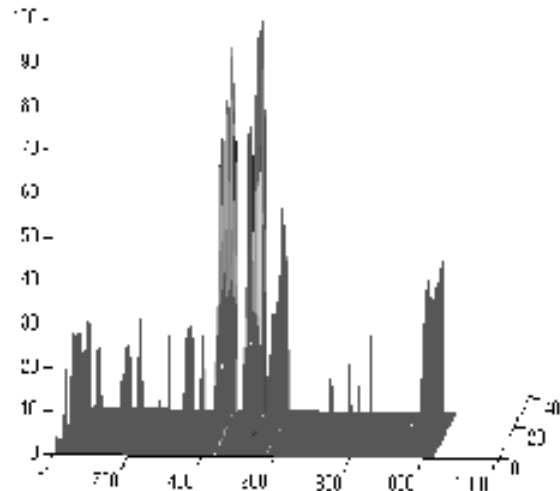


Fig. 11. 3_D processed spectra

Fig. 12 is the plot of one of the prediction frequency against spectral average number. When the average number is less than 15, the prediction frequency is serious fluctuation. When more than 20 spectra are averaged, the estimation result of the spectra is converged to a certain value. This result shows that the signal to noise ratio is improve significantly when more than 20 spectra are averaged.

5. CONCLUSION AND FUTURE RESEARCH

Our frequency estimation indicate that an accumulation of at least 20 single spectra is required to get a quality spectrum.

The table 1 shows the signal to signal ratio of original spectra and processed spectra obtained by three algorithms. The low pass filter algorithm gives the best result because of spectra characteristic of low frequency, although it is very simple algorithm.

Spectra	SNR (dB)
Original spectra	11.2
ALE algorithm	16.7
Autocorrelation scheme	15.4
Low pass filter scheme	24.3

Table 1

The distortion of spectral line is too serious with the method of adaptive line enhancer. Although the three peaks are enhanced, several small peaks appear around the bottom of the main peaks. This is not allowed for spectral analysis. The two parameter of a and L need to be modified to seek the possibility to reduce this distortion.

As we mentioned early, in this research, these PSD methods only apply to a simple sample, which is one element of Cr with three spectral lines. Next step, a more complicated sample with more lines may be used to test three DSP methods.

We will continue to develop new DSP technique.

REFERENCES

- [1] Dennis F. Flangan, Discrepancies between two formulations of signal-to-noise ratio for back-ground-limited detection. *Applied Optics*, Vol.34, No. 15, pp.2721-2723, May, 1995.
- [2] E. Damon and R. Thomlinson, "Observation of Ionization of Gases by a Ruby Laser", *Appl. Opt.* 2, 546 (1963).
[3] R. G. Meyerand and A. F. Haight, "Gas Breakdown at Optical Frequencies", *Phys. Rev. Lett.* 9, 401 (1963)
- [4] David A. Cremers and Leon J. Radziemski, "Laser Plasma for Chemical Analysis", *Laser Spectroscopy and Its Applications*, edited by Leon J. Radziemski, Richard W. Solarz and Jeffrey A. Paisner, Marcel Dekker, Inc., New York (1987)
- [5] M. M. Litvak and D. F. Edwards, "Spectroscopic Studies of Laser-Produced Hydrogen Plasma", *IEEE J. Quant. Electron.* QE-2, 486 (1966)
- [6] W. F. Braerman, C. R. Stumpell, and H. J. Kunze, "Spectroscopic Studies of a Laser-Produced Plasma in Helium" *J. Appl. Phys.* 40, 2549 (1969)
- [7] N. Ahmad, B. C. Gale, and M. H. Key, "Experimental and Theoretical Studies of the Time and Space Development of Plasma Parameters in a Laser Induced Spark in Helium", *Proc. R. Soc. London A301*, 231 (1969)
- [8] E. V. George, G. Bekefi, and B. Ya'akobi, "Structure of the Plasma Fireball Produced by a CO₂ Laser", *Phys. Fluids* 14, 2708 (1971)
- [9] P. de Montgolfier, P. Dumont, Y. Mille and J. Villermaux, "Laser-Induced Gas Breakdown: Spectroscopic and Chemical Studies", *J. Phys. Chem.* 76, 31 (1972)
- [10] R. W. Stevenson, "Spectroscopic Examination of Carbon Dioxide Laser-Produced Gas Breakdown", Thesis, Naval Postgraduate School, Monterey, California (1975)
- [11] Leon J. Radziemski, Thomas R. Loree, David A. Cremers, and Nelson M. Hoffman, Time-Resolved Laser-Induced Breakdown Spectroscopy of Aerosols", *Anal. Chem.* 55, 1246 (1983)
- [12] R. W. Schmieder, "Laser Spark: Focus on Combustion", *Sandia Technology* 5, 1 (1979)
- [13] D. K. Ottesen, J. C. F. Wang, and L. J. Radziemski, "Real-Time Laser Spark Spectroscopy of Particulates in Combustion Environments", *Appl. Spectrosc.* 43 967 (1989)
- [14] N. Wiener, *Extrapolation, Interpolation and Smoothing of Stationary Time Series, with Engineering Applications*. New York: Wiley, 1949.
- [15] H. Bode and C. Shannon, "A simplified derivation of linear least squares smoothing and prediction theory," *Proc. IRE*, vol. 38, pp.417-425, Apr. 1950.
- [16] R. Kalman, "On the general theory of control," in *Proc. First IFAC Congress*. London: Butterworth, 1960.
- [17] R. Kalman, and R. Bucy, "New results in linear filtering and prediction theory," *Trans. ASME, Ser. D. J. Basic Eng.*, vol. 83, pp. 95-107, Dec. 1961.
- [18] T. Kailath, "A view of three decades of linear filtering theory," *IEEE Trans. Inf. Theory*, vol. IT-20, pp. 145-181, Mar. 1974.
- [19] P. Howells, "Intermediate frequency side-lobe canceller," U.S. Patent 3,202,990, Aug. 24, 1965.
- [20] B. Widrow and M. Hoff, Jr., "Adaptive witching circuits," *IRE WESCON Conv. Rec.*, pt. 4, pp. 96-104, 1960.

- [21] J. Koford and G. Groner, "The use of an adaptive threshold element to design a linear optimal pattern classifier," *IEEE Trans. Inf. Theory*, vol. IT-12, pp. 42-50, Jan. 1966.
- [22] F. Rosenblatt, *Principles of Neurodynamics: Perceptrons and the Theory of Brain Mechanisms*. Washington, D.C.: Spartan Books, 1961.
- [23] D. Gabor, W.P.L. Wilby, and R. Woodcock, "A universal nonlinear filter predictor and simulator which optimizes itself by a learning process," *Proc. Inst. Electr. Eng.*, vol. 108B, July 1960.
- [24] R. Lucky, "Automatic equalization for digital communication," *Bell Syst. Tech. J.*, vol 44, pp. 547-588, Apr. 1965.
- [25] R. Lucky, J. Salz, and E. J. Weldon, Jr., *Principles of Data Communication*. New York: McGraw-Hill, 1968.
- [26] J. Kaunitz, "Adaptive filtering of broadband signals as applied to noise cancelling," *Stanford Electronics Lab., Stanford Univ., Stanford, Calif., Rep. SU-SEL-72-038*, Aug. 1972 (Ph.D. dissertation).
- [27] M. Sondhi, "An adaptive echo canceller," *Bell Syst. Tech. J.*, vol. 46, pp. 497-511, Mar. 1967.
- [28] J. Rosenberger and E. Thomas, "Performance of an adaptive echo canceller operating in a noisy, linear, time-invariant environment," *Bell Syst. Tech. J.*, vol. 50, pp. 785-813, Mar 1971.
- [29] B. Widrow et al., "Adaptive noise cancellation" principles and application," *proc. IEEE*, vol. 63, pp. 1691-1717, 1975.
- [30] S. J. Orfanidis, *optimum signal processing*, (2nd Edition, macmillan, New York, 1988).
- [31] P. M. Clarkson, *Optimal & Adaptive Signal Processing*, CRC press, 1993.
- [32] B. Widrow and S. D. Stearns, *Adaptive Signal Processing*, Prentice-Hall, NJ, 1985
- [33] L. Wang, N. H. Younan, and D. L. Monts, "On Using Adaptive Filtering to Extract the Absorption Cross Section of SO₂ in "DALAS" system," the 27th IEEE Southeastern Symposium on System Theory, 1995.
- [34] L.R. Rabiner, B. Gold and C.A. McGonegal, "An Approach to the Approximation Problem for Nonrecursive Digital Filter" *IEEE Trans. Audio and Electroacoustics* Vol. AU-18 pp83-106. June 1970.
- [35] John G. Proakis, Dimitris G. Manolakis, *Digital Signal Processing Principles, Algorithms, and Applications*, Macmillan Publishing Company, 1992.
- [36] S. Kay, *Modern Spectral Estimation: Theory and Application*, Prentice-Hall, NJ, 1987
- [37] S. Lawrence Marple, Jr, *Digital Spectral Analysis with Applications*, Prentice-Hall, NJ, 1987.